

CHAPTER 30

INTERFERENCE OF SMALL STRUCTURES IN THE VICINITY OF LARGE STRUCTURES

Subrata K. Chakrabarti, F. ASCE and Sumita Chakrabarti

Abstract



The purpose of this paper is to investigate the effect of large structures in the vicinity of small structures in the determination of wave forces on the small structures. The structures considered in this study are circular cylinders and analytical expressions are derived. It is shown that if the small cylinders are placed in close proximity of large cylinders (center distance/ caisson radius < 2.0), the wave forces on the small cylinder are largely influenced by the large cylinder.

INTRODUCTION

When large structures placed underwater encounter incoming waves, the waves alter in form in the vicinity of the structure. The problem is generally solved as a boundary value problem based on a linear velocity potential due to the incident wave. The diffraction effect of large coastal or offshore structures in waves is well-known. For an arbitrary shape of the structure the wave diffraction effect is solved numerically. For a fixed large caisson, this problem was solved by MacCamy and Fuchs (1955) in a closed form for Airy waves. This solution has been extended to the second-order wave theory [e.g., Molin (1979)]. For large cylinders in the vicinity of one another, the problem of multiple cylinder interaction is well-known [Chakrabarti(1978)]. In this case multiple diffraction from the neighboring cylinders is taken into account.

For structures which are placed near each other and are allowed to move independently, the problem of multiple radiation is taken into account in addition to multiple diffraction. Several research works addressed this problem in the diffraction regime, e.g., Ohkusu (1976).

The present study addresses the situation in which only one part of the structure is large enough to encounter diffraction effect. The other structure dimension is such that its effect on the waves is local and its presence has little influence on the large structure. Examples of such applications are composite structures, e.g., the Maurcen gravity platform in the North Sea and piles in the neighborhood of large caisson as shown in Fig. 1.

In this case, the small structure, such as, the pile, will experience a wave that is a combination of the incident wave and the scattered wave from the neighboring large structure. The size of the small structure is such that it falls in the Morison force regime in that both the inertia and drag effects are important.

¹Offshore Structure Analysis, Inc. 191 E. Weller Dr. North, Plainfield, IL 60544

²Biomedical Engineering Dept., Northwestern University, Evanston, IL 60201

Two different cases are considered in this study. In the first case, a pile is placed near a large caisson. Expressions of the forces on the pile are derived in the presence of the caisson based on the MacCamy-Fuchs theory. In the second case, the presence of large multiple cylinders on a small diameter member is investigated. Here, multiple scattering effect of waves on the small member is considered. An example of this situation may be found in the presence of multi-legged gravity offshore structure on risers.

Analytical solutions are derived for the total velocity potential at a point in the wave field which includes the wave scattering effect. The wave kinematics are derived based on this velocity potential. The forces on the small member are then expressed in terms of the wave kinematics. Numerical results are presented in all cases. Comparisons are made for the forces on the small structure with and without the presence of the large structure. In particular, the effect of spacing between the large and small structures is shown. The region where the influence of the large structure is significant in the design of the small structure is discussed.

LARGE VERTICAL CYLINDER

For a large vertical cylinder an analytical solution for the linear diffraction problem has been derived by McCamy and Fuchs (1954). In this case the expression for the incident wave is written in a convenient cylindrical polar coordinate (Fig. 1). The expression for the total potential at a point (r, θ) in the fluid field is obtained as

$$\Phi = \frac{H\omega}{2k} \frac{\cosh ks}{\sinh kd} \sum_{m=0}^{\infty} \delta_m i^{m+1} \left[J_m(kr) - \frac{J'(ka)}{H_m^{(1)'}(ka)} H_m^{(1)}(kr) \right] \cos m\theta \exp(-i\omega t) \quad (1)$$

in which H = wave height, ω = wave frequency, k = wave number, s = vertical distance from the ocean floor, d = water depth, a = caisson radius, and t = time. The quantities J_m and $H_m^{(1)}$ are the Bessel and Hankel functions of the first kind of order m respectively and prime denotes derivatives with respect to their arguments. Note that $H_m^{(1)} = J_m + iY_m$ where Y_m is the Bessel function of the second kind of order m . The value of δ_m is 1 for $m=0$ and 2 for $m>0$. The first term inside the bracket corresponds to the incident waves while the contribution of the scattered wave from the cylinder surface to the potential function is given by the second term within the bracket involving the Hankel function.

Note that while the above equation is written in complex form for mathematical convenience, only the real part of the expression matters. The horizontal water particle velocities are given in terms of Φ by

$$u_r = \frac{\partial \Phi}{\partial r} \quad (2)$$

and

$$u_\theta = \frac{1}{r} \frac{\partial \Phi}{\partial \theta} \quad (3)$$

Using the expression for Φ in Eqs. 2 and 3, we have

$$\bar{u}_r = \frac{\cosh ks}{\sinh kd} \sum_{m=0}^{\infty} \delta_m i^{m+1} \left[J_m'(kr) - \frac{J_m'(ka)}{H_m^{(1)'}(ka)} H_m^{(1)'}(kr) \right] \cos m\theta \exp(-i\omega t) \quad (4)$$

and

$$\bar{u}_\theta = -\frac{1}{kr} \frac{\cosh ks}{\sinh kd} \sum_{m=0}^{\infty} m \delta_m i^{m+1} \left[J_m'(kr) - \frac{J_m'(ka)}{H_m^{(1)'}(ka)} H_m^{(1)'}(kr) \right] \sin m\theta \exp(-i\omega t) \quad (5)$$

where bar denotes nondimensional quantities and the velocities are normalized by dividing by the quantity $(H\omega/2)$. In Cartesian coordinate system the horizontal particle velocity and acceleration components at the pile center are

$$\begin{aligned} \bar{u}_x &= \bar{u}_r \cos\theta - \bar{u}_\theta \sin\theta \\ \bar{u}_z &= \bar{u}_r \sin\theta + \bar{u}_\theta \cos\theta \\ \bar{\dot{u}}_x &= -i\omega \bar{u}_x \\ \bar{\dot{u}}_z &= -i\omega \bar{u}_z \end{aligned} \quad (6)$$

where the coordinate x is the direction of waves and z normal to this direction. The derivation thus far has been carried out in the complex field. However, in order to apply the expressions for the kinematics in the Morison force, it is necessary to use the real parts of these quantities. The forces on a unit section of the pile in the neighborhood of the single cylinder are computed based on these kinematics using the Morison equation. The forces along and transverse to the wave direction respectively are

$$\bar{f}_x(\omega t) = -\pi C_M \frac{D}{H} \operatorname{Re}\{\bar{i}\bar{u}_x \exp(-i\omega t)\} + C_D \left| \operatorname{Re}\{\bar{u}_x \exp(-i\omega t)\} \right| \operatorname{Re}\{\bar{u}_x \exp(-i\omega t)\} \quad (7)$$

and

$$\bar{f}_z(\omega t) = -\pi C_M \frac{D}{H} \operatorname{Re}\{\bar{i}\bar{u}_z \exp(-i\omega t)\} + C_D \left| \operatorname{Re}\{\bar{u}_z \exp(-i\omega t)\} \right| \operatorname{Re}\{\bar{u}_z \exp(-i\omega t)\} \quad (8)$$

in which D = pile diameter, C_M = inertia coefficient and C_D = drag coefficient. The forces in the above expressions are nondimensionalized by the quantity $1/2 \rho D (H\omega/2)^2$.

While the Morison equation in general will not produce a transverse horizontal force on a pile, the diffraction effect of the wave from the caisson is expected to introduce a transverse force.

Note that these expressions do not state anything about the vortex induced lift force as the Morison equation fails to describe this phenomenon. The description of the transverse force in this case is complicated by the fact that the scattered wave introduces a flow field which has a direction different from that of the incident wave and depends on the location of the fluid field.

It is considered interesting to compare these forces with the forces on the same pile in the absence of the large caisson. The force on the pile in the x-direction (Morison force is absent in the z-direction) written in the same nondimensional form is expressed as

$$\bar{f}_{xa} = -\pi C_M \frac{D}{H} \bar{u} \sin \omega t + C_D \bar{u}^2 |\cos \omega t| \cos \omega t \quad (9)$$

where the nondimensional force has the same form as in Eq. 7 and

$$\bar{u} = \frac{gk}{\omega^2} \quad (10)$$

This last quantity approaches a value of one in deep water.

LARGE MULTIPLE CYLINDERS

Assume that the pile resides in the neighborhood of a multi-legged vertical structure whose legs represent large vertical cylinders. The pile experiences multiple diffraction from these cylinders. The effect of the waves on the pile, as before, is considered small in developing the theory. Considering the interaction of the waves with all large cylinders in the flow field, the total potential is described with reference to the coordinate system described at the center of the δ th cylinder as

$$\Phi^\delta = \frac{iH\omega}{2k} \frac{\cosh ks}{\sinh kd} \left\{ \begin{array}{l} \sum_{n=-\infty}^{\infty} -J_n(kr_\delta) \exp(in(\theta_\delta - \theta_\omega + \pi/2)) \\ + A_n^\delta H_n(kr_\delta) \exp(in\theta_\delta) \\ + (\sum_{\mu=1}^{\delta-1} + \sum_{\mu=\delta+1}^{\Delta}) \sum_{m=-\infty}^{\infty} A_n^\mu H_{n+m}(kr_{\delta\mu}) J_m(kr_\delta) \\ \exp(im(\theta_{\delta\mu} - \theta_\delta)) \exp(in\theta_{\mu\delta}) \end{array} \right\} \exp(-i\omega t) \quad (11)$$

in which Δ = total number of large cylinders, θ_ω = angle of incident wave with respect to the positive x-axis, r_δ , θ_δ = location of field point with respect to the center of δ th cylinder (see Fig. 2). For convenience, the center of the coordinate system is located at the center of the caisson δ . To numerically compute the potential function, the infinite sums in the above equation are

replaced by a finite sum from -N to N where N is the number of symmetric images provided of the caisson in question. The first term within the bracket is due to the incident wave, the second term arises from the scattering from the reference δ th cylinder and is similar to the MacCamy-Fuchs expression. The third series term is due to scattering from the balance of the cylinders in the neighborhood where the Bessel's addition theorem has been used to transfer the coordinate system to the reference cylinder.

The expression for Φ^δ satisfies Laplace's equation and all boundary conditions except the cylinder surface condition. As for the single cylinder, when this condition is applied, a matrix equation in the unknown coefficients A_n^δ is derived.

$$\left. \begin{aligned} & \sum_{\mu=1}^{\delta-1} \sum_{m=-N}^N A_m^\mu H_{n+m}(kr_{\delta\mu}) \exp(im\theta_{\mu\delta}) J'_n(ka_\delta) \exp(in\theta_{\delta\mu}) + A_{-n}^\delta H'_{-n}(ka_\delta) \\ & + \sum_{\mu=\delta+1}^{\Delta} \sum_{m=-N}^N A_m^\mu H_{n+m}(kr_{\delta\mu}) \exp(im\theta_{\mu\delta}) J'_n(ka_\delta) \exp(in\theta_{\delta\mu}) \\ & = J'_{-n}(ka_\delta) \exp(ikr_{0\delta} \cos(\theta_{0\delta} - \theta_\omega)) \exp(-in(-\theta_\omega + \pi/2)) \end{aligned} \right\}, n = -N, \dots, N \quad (12)$$

In the above, the higher the value of N, the better is the accuracy in Φ^δ . The order of the matrix is given by $(2N+1)\Delta$. The coefficients A_n^δ are computed by the matrix inversion.

Once the velocity potential at a field point, r_δ, θ_δ is known, the particle kinematics are computed as before from Eqs. 2 and 3 so that the forces on the pile may be obtained from the Morison equation. The spatial part of the radial and tangential velocities at the center of the pile (r_δ, θ_δ) is obtained from

$$\bar{u}_r^\delta = i \frac{\cosh ks}{\sinh kd} \left\{ \begin{aligned} & \sum_{n=-N}^N -J'_n(kr_\delta) \exp(in(\theta_\delta - \theta_\omega + \pi/2)) + A_n^\delta H'_n(kr_\delta) \exp(in\theta_\delta) + \\ & \left(\sum_{\mu=1}^{\delta-1} + \sum_{\mu=\delta+1}^{\Delta} \right) \sum_{m=-N}^N A_m^\mu H_{n+m}(kr_{\delta\mu}) J'_m(kr_\delta) \exp(im(\theta_{\delta\mu} - \theta_\delta)) \exp(in\theta_{\mu\delta}) \end{aligned} \right\} \quad (13)$$

and

$$\bar{u}_\theta^\delta = \frac{-\cosh ks}{kr \sinh kd} \left\{ \begin{aligned} & \sum_{n=-N}^N -n J_n(kr_\delta) \exp(in(\theta_\delta - \theta_\omega + \pi/2)) + n A_n^\delta H_n(kr_\delta) \exp(in\theta_\delta) + \\ & \left(\sum_{\mu=1}^{\delta-1} + \sum_{\mu=\delta+1}^{\Delta} \right) \sum_{m=-N}^N A_m^\mu (-m) H_{n+m}(kr_{\delta\mu}) J_m(kr_\delta) \exp(im(\theta_{\delta\mu} - \theta_\delta)) \exp(in\theta_{\mu\delta}) \end{aligned} \right\} \quad (14)$$

It can be shown that for a two cylinder case, the total number of images $N=7$ provides sufficient accuracy (up to 4 significant digits) for forces. For symmetric two caisson/ one pile configuration

at right angles to the flow, the last two terms in the radial velocity expression u_r^6 should provide equal values at the pile. This provides a check on the numerical computation. Thus the transverse force will be absent in this case as one would expect.

NUMERICAL RESULTS

In order to show the effect of a single large caisson on the forces on a pile, numerical values on the forces on the pile are computed with and without the presence of the caisson. For this comparison the values of the hydrodynamic coefficients are taken as $C_M=2.0$ and $C_D=1.0$. The water depth to the caisson radius is taken as 1.0 and the forces are computed at the still water surface. The pile diameter to the wave height ratio is considered to be 0.25. In deep water this corresponds to a Keulegan-Carpenter value of about 12. Three different diffraction parameter values ka are chosen: $ka=1.0, 2.0, 3.0$. The pile is placed at different distances from the center of the caisson at 0, 90, and 180 degree orientation. Note that 0 degree corresponds to the pile placed behind the caisson with respect to the wave direction, 180 degrees places it in front of the caisson while 90 degrees is transverse to the flow.

The results for ka values of 1.0, 2.0 and 3.0 are shown in Figs. 3-5. The x-axis corresponds to the nondimensional distance r/a where r is the distance between the centers of the caisson and the pile and a is the caisson radius. The y-axis represents nondimensional force amplitudes on the pile. The quantities FX and FZ show forces in the presence of the caisson while FXA is the force in its absence. For the 0 and 180 degree cases only the x forces (FX) are presented as one would expect. However, for the 90 degree case, there is a force component in the z direction (FZ) as well.

The 0 degree case shows the shielding effect. When the pile is very close to the caisson the x force on the pile is small compared to the single pile case. As the pile is moved away from the caisson in the 0 degree direction, the x force on the pile increases and approaches in value to the single pile forces. This increase is slow and the forces are close to each other at a distance of six radius away.

When the pile is in front of the caisson facing the wave, the force on the pile is affected by the oscillating nature of the wave as the pile is moved away. The effect of the caisson here is high and is felt by the pile for a long time. Interestingly, the diffracted wave being out of phase with the incident wave, the forces experienced by the pile as it is moved away, fluctuates in magnitude, sometimes re-inforcing and sometimes canceling the single pile forces. This oscillation frequency corresponds to the wave length of the incident (and diffracted) wave.

When the pile is transverse to the caisson with respect to the wave direction, the wave load on the pile is considerably higher than the pile alone case due to closeness of the caisson. As in the 180 degrees case, the load fluctuates about the pile-alone force as the caisson is moved along the 90 degree line. The load approaches the pile-alone force with increasing distance. In fact, at a distance of about five times the radius, the forces are almost identical. This orientation also experiences a transverse load whose magnitude is as much as 25 percent of the single pile load.

The transverse load is small in the close proximity of the caisson and grows steadily with distance reaching maximum quickly near a distance of two radii.

As the diffraction parameter is increased in value (equivalent to higher wave frequency), the oscillation frequencies at 90 and 180 deg. increase. The normalized forces, however, are higher at the lower ka values.

A second numerical example shown here is the load on a pile in the presence of two large caissons symmetrically placed around the pile (Fig. 6). In this case the pile is always assumed to be in the center while the distance of the caissons from the pile is varied symmetrically. The normalized x and z loads on the pile are plotted in Fig. 7 for a ka value of 2.0. The loads at still water surface as before are shown and the values of C_M and C_D are taken as 2.0 and 1.0 respectively. The other values are the same as before. In this case, the transverse force is zero due to the symmetric configuration since the forces produced by the caisson no. 1 will be equal and opposite to the forces generated due to the presence of caisson no. 2. On the other hand, the x -force is considerably higher than the single pile force due to the re-inforcement caused by the caisson pair. For example, close to the caissons (r/a near 1.0), the force on the pile is more than twice that of the single pile.

CONCLUDING REMARKS

Analytical expressions have been derived on forces on piles in the presence of caissons. The theory is derived for a pile near a single caisson as well as near multiple caissons. Numerical values are given for several examples, including pile near a single caisson, and pile in the center of a caisson pair. Results show that the force is influenced by the presence of the caisson for $r/a < 2.0$. A transverse force is generated for a single caisson case at 90 deg. due to diffraction of waves. Multiple caisson interaction with the pile is more pronounced. Many offshore and coastal structures include the geometry presented in the above examples, e.g., Maureen Gravity Platform, Risers on Tension Leg Platforms, etc. where this interaction may be important.

REFERENCES

- Chakrabarti, S.K., "Wave Forces on Multiple Vertical Cylinders", Journal of the Waterway, Port, Coastal and Ocean Division, ASCE, Vol. 104, May, 1978, pp. 147-161.
- MacCamy, R.C. and Fuchs, R.A., "Wave Forces on Piles: A Diffraction Theory", Tech Memo No. 69, U.S. Army Corps of Engineers, Beach Erosion Board, 1957.
- Molin, B. "Second-Order Diffraction Loads upon Three-Dimensional Bodies", Applied Ocean Research, Vol. 1, No. 4, 1979, pp. 197-202.
- Ohkusu, M., "Ship Motions in Vicinity of a Structure", Proceedings of International Conference on the Behavior of Offshore Structure, Norwegian Institute of Technology, Trondheim, Norway, Vol. 1, 1976, pp. 284-306.

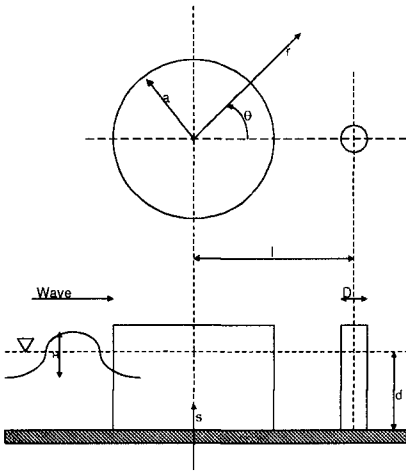


Fig. 1 Definition Sketch for Single Caisson

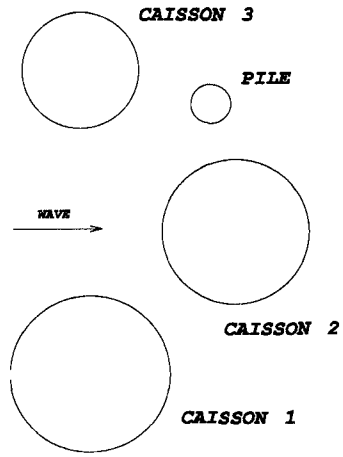


Fig. 2 Definition Sketch for Multiple caisson

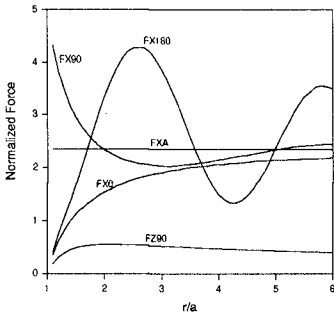


Fig. 3 Forces on Pile with and without Single Caisson -- $ka=1.0$

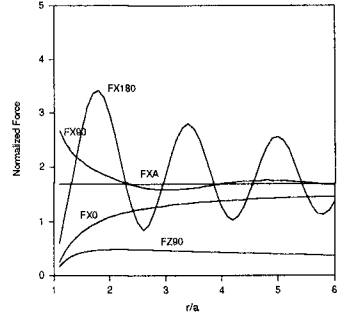


Fig. 4 Forces on Pile with and without Single Caisson -- $ka=2.0$

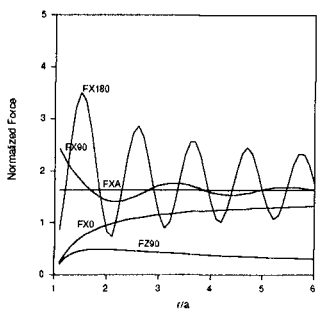


Fig. 5 Forces on Pile with and without Single Caisson -- $ka=3.0$

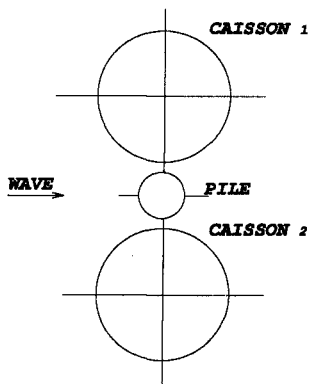


Fig. 6 Example Problem -- Pile in the Center of Two Caissons

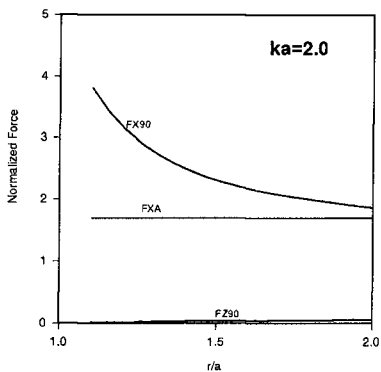


Fig. 7 Forces on Pile with and without Two Caissons -- $ka=2.0$